Santi *et al. Built Heritage* (2025) 9:63
https://doi.org/10.1186/s43238-025-00233-9

Built Heritage

RESEARCH ARTICLE

Open Access

The brick material culture of Urbino (UNESCO World Heritage, Central Italy) as inferred from a multidisciplinary archaeometric study on the historic architecture

Patrizia Santi[1*], Francesco Veneri[1], Gianluigi Tonelli[1], Mario Tramontana[1], Laura Panzeri[2], Anna Galli[2] and Alberto Renzulli[1]

Abstract

Roman to Modern times (19th century) brick samples from monuments, walls and other masonry buildings of the historic centre of Urbino were investigated through a multidisciplinary approach, including mineralogy and texture (thin section and XRPD), chemistry (major-trace elements), physical–mechanical properties and thermoluminescence (TL) dating, coupled with the historic literature data. TL mostly confirms the building periods of the architectural structures where the bricks were sampled, also emphasising for the Cathedral a building period that lasted more than three centuries. The supply areas of the raw materials seem to have always been the same through time, very close to the city to the West and Northwest, represented by the deposits deriving from the weathering of the Marnoso-Arenacea Formation, which was able to give both clays and sands (temper) for the bricks. Some historic documents of the second half of the 15th century reporting an act of sale of a person living in the western areas surrounding Urbino with a commitment to providing several thousand of bricks to the Cathedral factory, seem to confirm the geological constraints. The firing temperature should have been reached at least 850–900°C, as indicated by the presence of new phases such as gehlenite and clinopyroxene in almost all the investigated samples. Nevertheless, the failure to achieve complete thermodynamic conditions for both wide inhomogeneities in grainsize and composition of the raw materials and the lack of temperature control during firing, mostly gave rise to incomplete calcite breakdown. The absence of standardisation of the pyrotechnological processes probably led to the large variability of the physical–mechanical features even for bricks of the same building period. Uniaxial Compressive Strength of the investigated historic bricks, however, falls within the range of present-day full-bricks, and a general improvement of the brick quality from Roman to Modern times was highlighted, as well as a progressive refinement in preparation techniques before firing. The brick material culture of Urbino continues seamlessly, after the investigated periods, until the second half of the 20th century, testified by the presence of the brick factory of the *Fornace Volponi*, just outside the historic centre of the city.

Keywords Bricks, Mineralogy, Chemistry, Physics, TL dating, Raw materials, Cultural heritage

*Correspondence:
Patrizia Santi
patrizia.santi@uniurb.it
[1] Dipartimento di Scienze Pure e Applicate, Campus Scientifico E. Mattei, Via Cà Le Suore 2-4, Università degli Studi di Urbino Carlo Bo, Urbino 61029, Italy
[2] Dipartimento di Scienza dei Materiali, Via R. Cozzi, 55 - Università degli Studi di Milano Bicocca, Milan 20125, Italy

1 Introduction

1.1 Town's founding, growth and architectural framework

The historic centre of the city of Urbino develops between two hills: *San Sergio* to the North and *Poggio* to the South (Figs 1 and 2a). Upon this latter hill (460 m a.s.l.), characterised by natural defensive slopes and a water spring (Luni and Ermeti 2001), ancient peoples established their settlements. The saddle between the two hills successively became the heart of the Renaissance and Baroque architecture of the town.

Starting from the fourth century BCE, with *Galli Senoni,* and successively with the Romans, from 285 BCE up to 476 CE, the *municipium* of *Urvinum Mataurense* (Agnati 1999) developed. The ancient Roman city (*oppidum*) was protected by defensive walls all around the hill and a relatively small plain (third-second century BCE; Luni and Ermeti 2001). Some visible remains of this period are the theatre, small tracts of defensive walls with traces of their gates, and, external with respect to the Roman city, a monumental tomb (TRC1 and TRC2 brick samples in the present work) and a kiln (FRP1 and FRP2 samples) in the southern and northern surroundings, respectively (Fig. 2a,b). In the following centuries (Medieval Period), the urban settlement developed towards the northern hill of *San Sergio*, resulting in the presence of the episcopal church, water containers and burial places (Luni 1986). In this period, a new system of defensive walls that redraw the same perimeter of the Roman ones, but expanding the area, was built, and the displacement of the cathedral from *San Sergio* within the city walls (11th century; Luni 1985) gave a new impulse to the urban development. Between the twelfth and thirteenth centuries, different districts developed all around the Roman road axis with the building of a new system of defensive walls (Mazzini 1982; Luni and Ermeti 2001; Negroni 2005). These latter ran around the city, parallel to the ancient Roman walls. In the same time the Montefeltro family took over the city government (1234 CE). In the eastern sector of the city, a convent of Augustinian nuns was founded (1320s; Ligi 1938) in correspondence with a tower of the Medieval walls (*Santa Maria della Torre*, SMT1, SMT2, SMT3, SMT4 samples; Fig. 2a,c) and the Dominican Convent of *Santa Chiara* was built (14th century, SC1 sample; Fig. 2a). An important structure made of bricks is the Albornoz Fortress (14th century; FA1 and FA2 samples; Fig. 2a,d). The Renaissance Period represented a fundamental urban evolution with the massive rebuilding of the city, mostly using bricks in several palaces. During the second half of the 15th century, the architects Luciano Laurana and Francesco di Giorgio Martini built the famous Ducal Palace of Duke Federico III da Montefeltro, partially including the existing medieval structures, thus becoming the new focus of the urban fabric. In the 16th century, new wide defensive walls encircled the expanded centre of the city (Luni and Ermeti 2001). In this period, a strong work of urbanisation, with the demolition of houses for new streets and squares, the building up of the Ducal Palace and the renovation of some churches and palaces took place (Negroni 2005). Concerning the construction of the Cathedral, it began in 1474, very close to the Ducal Palace in an area of pre-existing buildings. However, its building history lasts for more than three centuries, mostly because earthquakes during the 18th century which affected the structure, even with some collapses. In the present work, brick samples of the Cathedral (from DUM1 to DUM7; Fig. 2a,e) therefore represent different stages of building.

1.2 Bricks as part of the material culture of Urbino

The historic centre of Urbino is also known as the "city of bricks" (Baldi 1580; Siekiera 2010; Mazzini 1982) and in the World Heritage List (UNESCO 1998), it has been described as a city whose urban development has "harmoniously adapted to its physical site and its medieval precursor in an exceptional manner". This study, based on a multidisciplinary approach, was applied to some

Fig. 1 Panoramic view (from South-West) of the Urbino historic centre (Source: courtesy of Paolo Mini)

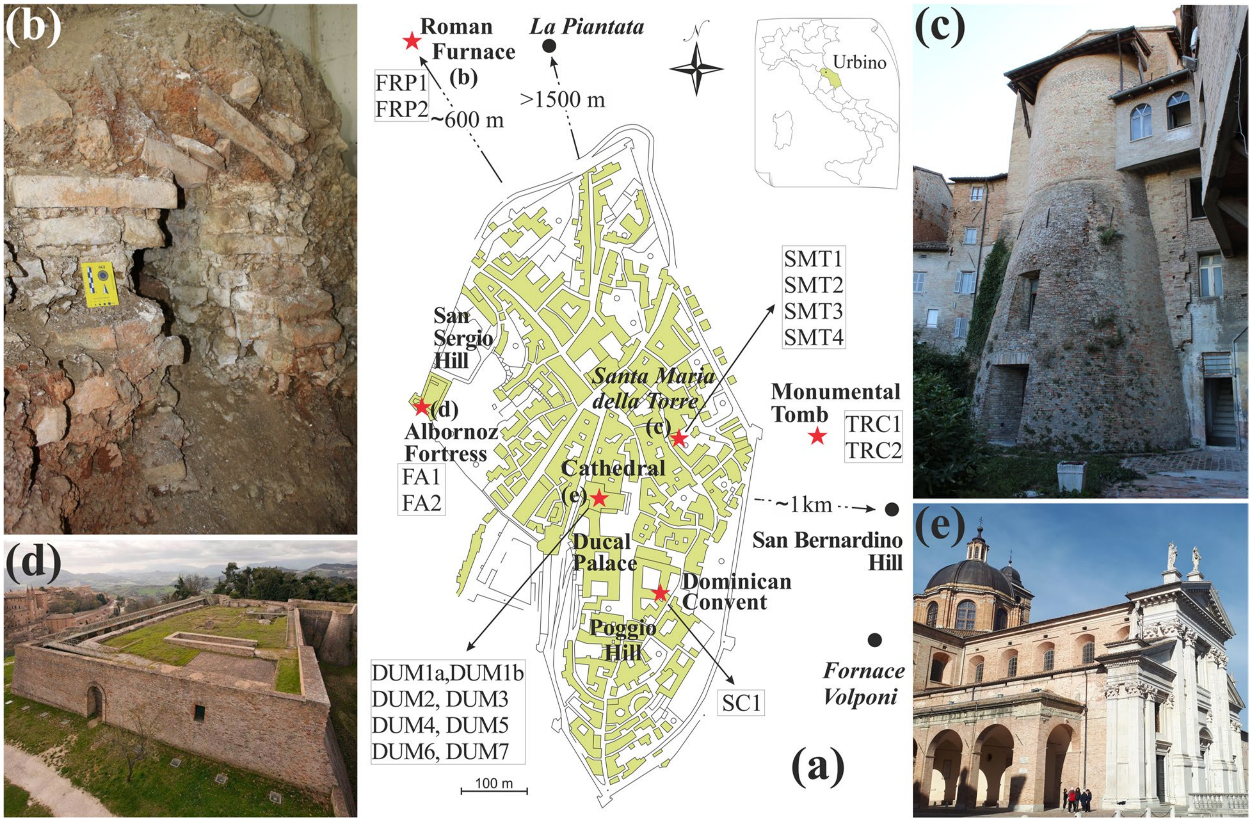

Fig. 2 Map of the historic centre of Urbino with: (**a**) the location of sampling of the bricks (red stars); (**b**) remnants of the Roman furnace (FRP); (**c**) Medieval rampart walls of *Santa Maria della Torre* church (SMT); (**d**) Medieval Albornoz Fortress (FA); (**e**) Cathedral (DUM) (Source: the authors, except for **d** which is courtesy of Paolo Mini)

historic bricks describing their texture, mineralogical and chemical composition, the pyrotechnology, the physical–mechanical properties and the thermoluminescence dating (TL), also focusing on the relative raw materials. The architectural history of Urbino is marked by the employment of bricks starting from the Roman Period, during which the pioneer architectural work of Vitruvius (Rowland and Howe 1999) can be considered the primary source of information concerning building techniques. In this extensive treatise of 10 books, Vitruvius not only illustrated building techniques and architectural theories but also extensively described the nature and preparation of the construction materials, including bricks, mortars and binders (Artioli et al. 2019). The presence in the territory of Urbino and, in general, in Central Italy, of good quality raw geomaterials such as clays (as binder) and sandstones (as temper) to make bricks, undoubtedly represented the background for their production. The warm orange-red colour of the bricks characterises most of the historic buildings of Urbino as well as those of many other cities of Central Italy (Marche, Umbria and Tuscany Regions).

Starting from the Romans to the Medieval Period, local production of bricks, most probably in rural areas near streams and small rivers around Urbino was developed for architectural purposes (Falcioni et al. 2024). Then, during the Renaissance, the architectural framework of Urbino spread using bricks for building several palaces, churches and defensive walls. Bricks were masterfully integrated with laths and blocks of local building stones in several monuments throughout the historic centre (Santi et al. 2019; 2021), included the Ducal Palace, which is the recognised symbol of the Renaissance architecture of the city. Literature studies concerning the bricks of the historic building of Urbino are relatively few. Luni and Ermeti (2001) deal with the use of bricks in archaeological contexts, whereas Busdraghi et al. (1992) carried out mineralogical and chemical analyses of bricks used in the Ducal Palace and the relative raw materials. Our analytical approach focuses on how the archaeometric investigations of the bricks from the architecture built in the city (using mineralogical, geological, chemical and physical methods) can constrain the brick material culture of Urbino as a whole, from the raw materials to the manufacturing through time, enhancing the valorization

Table 1 Summary of the sampled bricks and relative analyses

Sample	Site	TSA	XRPD	BCA	TL	PMP
	Roman Period (RoP)					
TRC1	Ruins of tomb	X	X	X		X
TRC2	Ruins of tomb	X				X
FRP1	Remnants of kiln	X	X	X	X	X
FRP2	Remnants of kiln (tile)	X	X	X	X	X
	Late Medieval Period (LMeP)					
SMT1	Medieval tower walls	X	X	X	X	X
SMT2	Medieval tower walls (southern face)	X	X	X	X	
SMT3	Medieval tower walls (northern face)	X	X	X		X
SMT4	Medieval tower walls (left side of tower)	X	X	X		X
FA1	Albornoz Fortress (eastern internal walls)	X	X	X	X	X
FA2	Albornoz Fortress (lower external walls)	X	X	X		X
SC1	Ex Dominican Convent	X	X	X		
	Renaissance Period (ReP)					
DUM1a	Cathedral (drill core at 60 cm depth of the third column of the left nave)	X	X	X	X	
DUM1b	Cathedral (drill core at 140 cm depth of the third column of the left nave)				X	
DUM2	Cathedral (tympanum of the pediment of the façade)	X	X	X		
	Modern Period (18th—19th century; MoP)					
DUM3	Cathedral (drill core n.2 at 80 cm depth of the drum of the dome)	X				X
DUM4	Cathedral (drill core n.4 at 40 cm depth of the drum of the dome)	X	X	X	X	X
DUM5	Cathedral (drill core n.1 at 120 cm depth of the drum of the dome)	X	X	X	X	X
DUM6	Cathedral (drill core n.3 at 35 cm depth of the drum of the dome)	X				X
DUM7	Cathedral (drill core of the drum of the dome)	X				X

Abbreviations: TSA Thin Section Analyses, *XRPD* X Ray-Powder Diffraction Analyses, *BCA* Bulk Chemical Analyses, *TL* Thermoluminescence dating, *PMP* Physical–Mechanical Properties

of the cultural heritage of the UNESCO historic centre of Urbino.

2 Materials and methods

2.1 Sampling

The analysed bricks come from architectural structures which are representative of different historic building periods of Urbino, and referable to four important edification phases of the city (Fig. 2, Table 1): Roman Period (RoP), Late Medieval Period (LMeP), Renaissance Period (ReP) and Modern Period (MoP). The sampling was carried out, after having considered the bibliographic historic data concerning the main architectonic structures, by collecting (*i*) fragments of already damaged bricks, which could not be reused (or integrated) for future restoration or (*ii*) from drill cores of the Urbino Cathedral available because of current restoration works of this monument after the earthquake of the Umbria-Marche-Lazio regions in 2016 (Fig. 3). For these reasons and the scarcity of some samples, different analyses were planned following a hierarchical strategy, to obtain a general investigation for the 19 collected bricks (see Table 1 for type of analyses carried out on each sample).

For the Roman Period, we sampled bricks of some in situ structures (Mercando 1985; Ermeti 1993; Luni and Ermeti 2001): the ruins of a monumental tomb (TRC1 and TRC2) and the remnant walls of a kiln (FRP1 and FRP2; Fig. 2b), both located in the surroundings of the historic centre of Urbino (Fig. 2a,b). The tomb, located not far from the Roman walls, in an area used as a necropolis, was discovered in 1972 and related to the first-second century (Luni 1985). Concerning the kiln ruins, they were discovered in 1990, because of public street restoration works. Ermeti (1993) suggests that some local production of ceramics, dating back to the third century, come from this kiln. The samples of the Late Medieval Period (Fig. 2a,c,d) are representative of three different architectural structures. These are (*i*) the rampart over which the church of *Santa Maria della Torre* was built (SMT1, SMT2, SMT3, SMT4; Fig. 2a,c); (*ii*) the base of the walls of the Albornoz Fortress (FA1 and FA2; Fig. 2a,d); (*iii*) the outer walls of the ex-Dominican Convent (SC1; Fig. 2a). The *Santa Maria della Torre* church was built in 1320 and its name derives from the ancient rampart, still well preserved, belonging to the medieval walls (Luni and Ermeti 2001) on which it was

Fig. 3 Sampling of the brick drill cores of the Cathedral during the restoration works after the 2016 earthquake. **a** View towards the entrance, in this way the pillars of the left nave are on the right and *viceversa*. (**b**) and (**c**) detail of the third pillar of the left nave, where the drill core of the samples DUM1a and DUM1b is shown. **d**, **e** and **f** details of the drill cores in three different parts of the drum of the dome (DUM5, DUM3 and DUM4) (Source: the authors)

directly built upon. The Albornoz Fortress was built for defensive purposes on top of the *San Sergio* hill in the second half of the 14th century by Anglico de Grimoard (Mazzini 1982). The name of the fortress come, however, from Cardinal Albornoz who planned a new defensive structure for the city (Luni and Ermeti 2001). Finally, sample SC1 is a fragment of a brick belonging to the remains of the perimeter walls of the former Dominican Convent (once located in Via *Santa Chiara*; Fig. 2a) whose origin is of uncertain date, around the middle of 1300. In 1847 the Dominican Convent was suppressed by Pope Pius IX for the construction of the Seminary Palace (Mazzini 1982). Only a part of the eastern perimeter walls is now recognisable. The bricks of the Renaissance and Modern Periods (Fig. 2a,e) are represented by samples collected in different sites of the Urbino Cathedral (third pillar of the left nave, tympanum of the pediment of the façade and drum of the dome; DUM1a, DUM1b, DUM2, DUM3, DUM4, DUM5, DUM6 and DUM7; Table 1 and Fig. 3). Concerning brick samples of the Cathedral deriving from the same pillar, it is worth noting that they were drilled at different depths: DUM1a at 60 cm and DUM1b at 140 cm from the present day wall of the pillar itself (Fig. 3a,b,c). All the bricks from the Modern Period building of the Cathedral also come from drill cores (Table 1; Fig. 3). The Cathedral started to be built on May 20, 1439 (Negroni 1993) based on the original project of Francesco di Giorgio Martini. Unfortunately, some earthquakes damaged different sectors of the architectural structures leading to the end of the works after more than three centuries. Major seismic events dating back to 1741 and 1781, were documented until that occurred in 1789 (Rovida et al. 2022) causing the dome's collapse. The completion of the church was assigned to the architect Giuseppe Valadier, who employed, in addition to the use of bricks, a local white

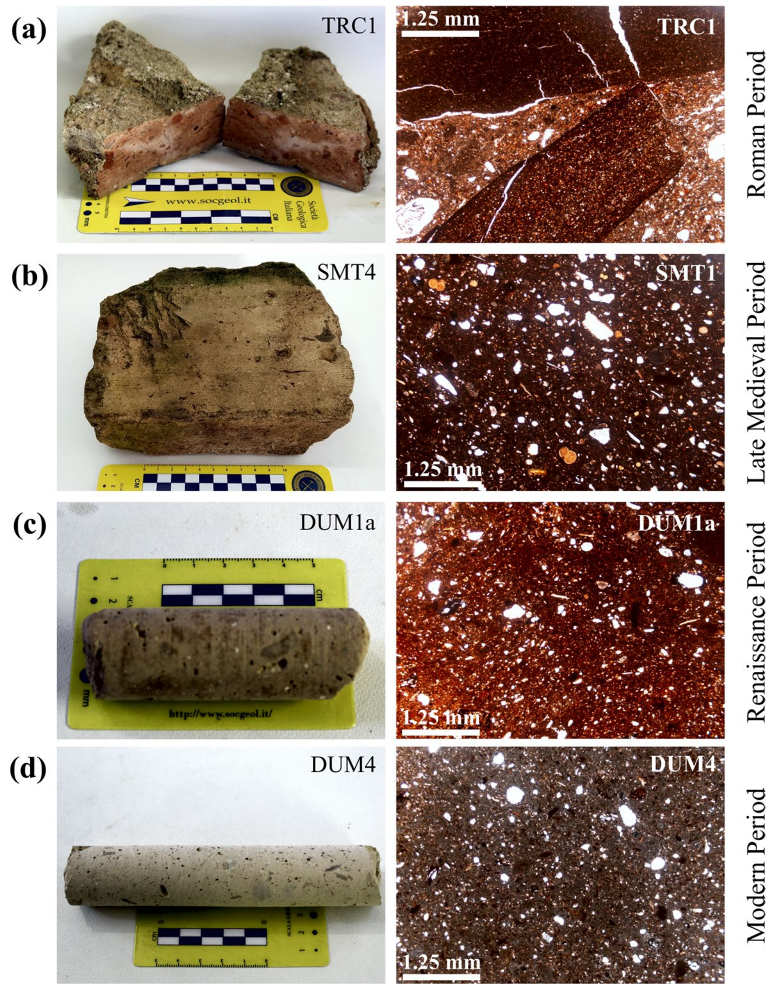

Fig. 4 Macroscopic and microscopic features of representative analysed bricks: (**a**) monumental tomb, (**b**) rampart of the *Santa Maria della Torre* church; (**c**) drill core of a pillar and (**d**) drum of the dome of the Cathedral (Source: the authors)

calcareous stone of the Jurassic Bugarone Group (Santi et al. 2021) for the façade. The Cathedral underwent the last restoration work after the last seismic events of 2016, with the Engineer Diego Talozzi in charge of the project that allowed us to collect some bricks, especially those from the drill cores (Fig. 3; Table 1).

2.2 Mineralogical, textural and chemical analyses

Texture and mineralogy on thin section of 18 out of 19 brick samples (Table 1 and Figs. 4 and 5) were described by Optical Polarizing Microscopy (OPM). Detailed mineralogy was also performed on 14 samples by X-Ray Powder Diffraction analyses (XRPD) using a Philips PW1830/3710, Cu Kα radiation, 35 kV, 30 mA diffractometer at the University of Urbino (Table 2; Supplementary Material 1, SM1). Major (wt.%) and trace (ppm) elements bulk chemical analyses (BCA on 14 samples; Table 3) were determined by ICP-OES (Inductively Coupled Plasma-Optical Emission Spectrometry) and ICP-MS (Inductively Coupled Plasma-Mass Spectrometry), respectively, at the Activation Laboratories LTD (Ancaster, Canada). The analytical procedure followed by the laboratory includes crushing and powdering samples in an agate mortar to avoid contamination as much as possible and fusing by a lithium metaborate/tetraborate technique in an induction furnace, providing a fast and high-quality fusion. The resulting molten bead was rapidly digested in a weak (5%) nitric acid solution containing an internal standard and mixed continuously until completely dissolved. Major oxides, including SiO_2, refractory minerals (*i.e.* zircon, sphene, chromite, etc.), REE and other high field strength elements are guaranteed to entry into solution by the method of attack used by Activation Laboratories LTD. Certified reference

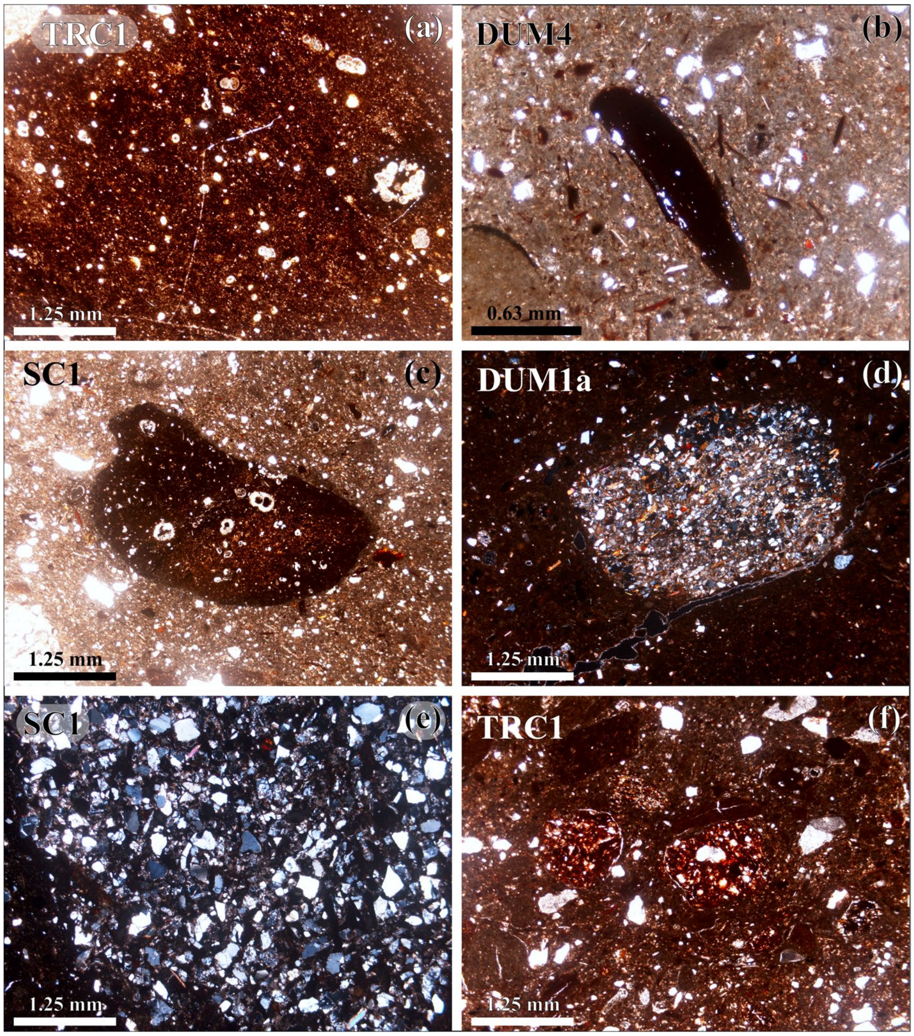

Fig. 5 Thin section microphotographs of representative textures and types of components. **a**, **b** and **c** pelitic/marly lumps; (**d**) and (**e**) medium-siltites to coarse-grained arenites respectively; (**f**) rounded ARFs fine-grained fragments. Images a,b,c,f were taken at plane-polarized light, d, e with crossed nicols (Source: the authors)

materials (www.actlabs.com) were used for the best calibration of chemical analyses. Errors, for major oxides and trace elements, are generally < 2% and < 5%, respectively and were calculated through both the use of certified natural rock standards and some replicates of samples. The detection limit is reported in Table 3 for each analysed element.

2.3 Thermoluminescence dating

Thermoluminescence dating (TL) is a well-known method used to establish the firing age of the bricks (Martini and Sibilia 2001). For the 9 samples analysed through TL (Table 4), the polymineral fine grain technique (4–11 µm; Aitken 1985; Zimmermann 1971) and the Multiple Aliquot Additive Dose (MAAD) protocol to evaluate the Equivalent Dose (De), were applied. TL dating was performed using a homemade system equipped with a photomultiplier tube (EMI 9235QB) coupled to a blue filter (Corning BG12) at the LAMBDA Laboratory of the Department of Materials Science of the University of Milano-Bicocca. The samples were heated from RT (Room Temperature) to 480 °C with a heating rate of 15 °C s^{-1}. Artificial irradiations were carried out using a 1.85 GBq ^{90}Sr-^{90}Y beta source (dose-rate: 3.33 Gy min – 1) and a 37 MBq ^{241}Am alpha source (dose-rate: 14.8 Gy min^{-1}).

The annual dose rate was indirectly determined from the measurement of the sample radioactivity. The concentrations of U and Th were obtained through total alpha counting using ZnS scintillator discs, assuming a

Table 2 Semi-quantitative mineralogical composition by XRPD

Sample	Qtz	Cal	Feld	Cpx	Ill/Mi	Wo	Gh	Gp	Ze
Roman Period (RoP)									
TRC1	XX	XXX	XX	X	XX		X		
FRP1	XX	XXX	XX	X	tr				
FRP2	XX	XXX	XX	X	X				
Late Medieval Period (LMeP)									
SMT1	XX	XXX	XX	tr	XX		tr		
SMT2	XX	XX	XX	XX			tr	XX	
SMT3	XX	XXX	XX	XX			X		
SMT4	X	XXX	XX	XX			X		XX
FA1	XX	XXX	XXX	tr	XX				
FA2	XX	XXX	XX	X	XX		X		
SC1	XX	XXX	XX	XX	X		X	XX	
Renaissance Period (ReP)									
DUM1a	XX	XXX	XX	X	XX		X		
DUM2	X	tr	XX	XXX		tr	X		
Modern Period (MoP)									
DUM4	X	tr	XXX	XXX		tr	X		
DUM5	XX	XXX	XX	X	XX				

Abbreviations: *Qtz* quartz, *Cal* calcite, *Feld* feldspar, *Cpx* clinopyroxene, *Ill/Mi* illite/mica group, *Wo* wollastonite, *Gh* gehlenite, *Gp* gypsum, *Ze* zeolite. Abundances: tr = traces, X = present, XX = abundant, XXX = very abundant

Th/U concentration ratio of 3.16 (Aitken 1985). The contribution from ^{40}K was derived from the total concentration of K measured by flame photometry. Since alpha particles are less effective in inducing luminescence compared to beta and gamma radiation, this was accounted for by determining the *a*-value, which is based on the comparison of luminescence signals induced by alpha and beta irradiations in the laboratory. Given that water absorbs part of the radiation that would otherwise reach the sample, the saturation water content was assessed for each brick. The F value (*i.e.*, the fraction of saturation corresponding to the assumed average water content) was taken as 50 ± 10% for all samples, based on available humidity data for the investigated area. Finally, the contribution of cosmic rays to the total dose rate was also taken into account (Prescott and Hutton 1994).

2.4 Physical–mechanical analyses

The physical and mechanical characterisation was carried out at the University of Urbino (Table 5). Due to the small size of the available samples it was possible to prepare parallelepiped specimens (2.5 to 5 cm for the base and 4 to 7 cm for the height) required for physical–mechanical testing, only for 14 bricks. The index properties (dry bulk density γd, specific gravity γs, total porosity n) were determined using the related standards (ISRM 1981). The uniaxial compressive strength σ (UCS; ISRM 1979) has been tested by a gradual increase of a compressive load up to the failure of the sample and represents the ratio of the failure load (F) and its cross-sectional area (A) before testing and it was evaluated following the procedure described in EN 1926 (2007).

3 Results

3.1 Macroscopic features, texture and mineralogy on thin section

Macroscopic observations of slices, cut parallel to the thickness of bricks, reveal differences in colour, structure, and components. The colour represents an important physical feature of fired clay bricks, depending on the chemical composition of the raw materials used and the firing processes. As a rule, brick colour is determined by the iron and the calcium carbonate contents of the raw materials and the presence of organic matter, combined with the amount of oxygen (redox conditions) in the furnace (Ashurst and Ashurst 1988). In our case, most of the bricks are orange (5YR 7/4; Munsell 1994) and show, progressively, an increasing colour homogeneity passing from Roman bricks (Fig. 4a) to the Late Medieval (Fig. 4b), Renaissance (Fig. 4c) and Modern Periods (Fig. 4d) ones. These two latter periods are characterised by lighter yellowish bricks (7.5YR 8/2–3; Munsell 1994; Fig. 4c,d). Zoning in colour is typically well visible in the Roman bricks, showing banded fluidal structures (Fig. 4a). In all the investigated bricks, apparent saline

Table 3 Whole-rock chemical composition (major and trace elements) of the analysed bricks; DL = Detection Limit

wt%	RoP			LMeP							ReP		MoP		
	TRC1	**FRP1**	**FRP2**	**SMT1**	**SMT2**	**SMT3**	**SMT4**	**FA1**	**FA2**	**SC1**	**DUM1a**	**DUM2**	**DUM4**	**DUM5**	**DL**
SiO_2	44.51	49.76	47.39	42.76	40.22	46.72	43.15	43.29	45.66	44.95	42.4	53	47.78	48.85	0.01
Al_2O_3	13.07	14.1	13.42	10.7	11.78	12.5	12.24	12.02	13.05	13.21	12.2	14.2	13.85	11.09	0.01
$Fe_2O_{3\ tot}$	5.06	5.56	5.45	4.52	4.81	4.86	4.59	4.65	5.09	5.19	4.98	5.43	5.77	4.22	0.01
MnO	0.11	0.10	0.11	0.10	0.13	0.17	0.09	0.09	0.10	0.12	0.15	0.17	0.13	0.08	0.005
MgO	3.97	3.47	3.21	3.97	5.9	4.97	3.97	3.03	3.51	3.93	3.82	4.58	4.86	3.76	0.01
CaO	17.84	13.72	12.17	17.73	16.66	18.96	22.35	16.59	16.51	19.35	16.41	16.85	21.54	12.99	0.01
Na_2O	0.78	1.13	1.13	1.13	1.2	1.36	1.76	1.04	1.19	1.03	1.04	1.29	1.18	1.36	0.01
K_2O	2.39	2.91	2.35	2.57	2.02	2.53	1.56	2.61	3.18	2.85	2.76	3.33	2.5	2.37	0.01
TiO_2	0.57	0.64	0.61	0.54	0.52	0.55	0.54	0.51	0.57	0.56	0.54	0.62	0.65	0.50	0.001
P_2O_5	0.15	0.16	0.13	0.14	0.12	0.13	0.15	0.12	0.16	0.17	0.12	0.15	0.14	0.12	0.01
LOI	12.2	8.84	13.67	16.2	16.6	7.55	10.02	16.57	10.35	8.6	16.01	1.05	1.48	13.44	
Total	100.6	100.4	99.64	100.3	99.94	100.3	100.4	100.5	99.37	99.96	100.4	100.7	99.88	98.77	
CaO + MgO	21.81	17.19	15.38	21.7	22.56	23.93	26.32	19.62	20.02	23.28	20.23	21.43	26.4	16.75	
ppm															
V	76	100	89	92	91	108	85	103	99	104	110	116	116	84	5
Ba	445	466	561	324	311	376	395	462	512	388	360	492	387	341	2
Sr	446	308	347	472	450	441	540	388	496	407	453	409	495	293	2
Y	21	26	25	23	23	22	22	19	21	22	21	25	24	18	1
Zr	100	134	129	145	100	111	119	99	112	106	105	137	127	122	2
Cr	110	120	110	80	100	110	100	100	90	110	90	130	130	80	20
Co	15	15	16	12	15	14	14	13	15	15	15	18	16	11	1
Ni	70	70	70	60	70	70	60	60	70	70	70	80	80	50	20
Cu	40	40	30	30	30	40	40	30	40	40	40	40	40	30	10
Rb	91	116	104	102	66	124	134	119	120	109	107	148	146	116	2
Nb	11	12	11	10	10	10	11	10	11	11	11	12	12	10	1
La	28.1	33.5	31.9	28.4	28.4	27.4	27.6	27.3	27.4	27.3	26.1	32.2	31.5	25.1	0.1
Ce	54.6	64.6	63.7	56	52.6	53.2	54.3	52.8	53.9	53.7	51.1	63.5	62.3	49.1	0.1
Nd	24.6	30.3	29	25.4	24.1	23.9	24.8	23.8	24.8	24.4	22.8	28.5	27.8	22.2	0.1
Sm	5	6.2	6	5.1	4.9	4.9	4.9	4.7	5	4.9	4.7	5.7	5.9	4.6	0.1
Eu	1.01	1.35	1.16	1.08	1.05	0.98	1.01	0.96	1.02	1.01	0.94	1.18	1.15	0.91	0.05
Gd	4.2	5.4	5	4.7	4.3	4.3	4.4	4.2	4.4	4.4	4.1	5.1	5	3.9	0.1
Dy	3.9	4.8	4.7	4.3	4.1	3.8	4	3.8	4.1	4	3.7	4.7	4.8	3.7	0.1
Ho	0.7	0.9	0.9	0.8	0.8	0.7	0.7	0.7	0.8	0.8	0.7	0.9	0.9	0.7	0.1
Pb	22	25	21	20	19	19	19	21	21	21	22	12	25	19	5
Th	9.7	11.2	10.8	9.6	9	9.3	9.5	9.6	9.8	9.9	9.3	11.1	11.1	8.6	0.1
U	3	2.8	2.5	3	2.6	2.9	4	2.9	2.8	2.9	2.7	3.3	3.2	2.6	0.1

crusts (*i.e.* efflorescences) and/or biological attacks have never been recognised.

Thin section analyses under the OPM emphasise inhomogeneities among samples of the different historic periods (and at places of the same period itself). The groundmass of the plastic binder shows a texture ranging from anisotropic optically active (only Roman bricks) to semi-isotropic optically active to inactive in the other samples. Microfossil species (*e.g. Foraminifera*) were also detected in both the groundmass and the pelitic/marly lumps (Figs. 4b and 5a,c). Microporosity and withdrawal micro-fissures are also present. Concerning the temper, grainsize inhomogeneity (poor sorting; Fig. 4) is a common feature of all the investigated bricks. Nevertheless, a decrease of both temper percentage and its average grainsize (vol.%) is shown passing from RoP to MoP bricks (Fig. 4a,b).

Minerals such as mono- and poly-crystalline quartz, K-feldspar, plagioclase, biotite, muscovite and opaque

Table 4 TL dating

Sample	Sat. Water content % ± 25%	^{238}U (ppm) ± 5%	^{232}Th (ppm) ± 5%	^{40}K (ppm) ± 3%	Annual Dose (mGy/y)	Equivalent Dose (Gy)	Dating CE
DUM4 (MoP)	20	2.8	8.85	2.82	10.4 ± 0.3	2.3 ± 0.3	1800 ± 40
DUM5 (MoP)	16	2.08	6.56	2.73	4.5 ± 0.1	1.1 ± 0.2	1780 ± 50
DUM1a (ReP)	12	2	6.3	3.06	6.1 ± 0.2	2.8 ± 0.5	1560 ± 90
DUM1b (ReP)	17	2.96	9.36	2.33	6.6 ± 0.2	3.7 ± 0.4	1460 ± 80
FA1 (LMeP)	12	1.86	5.87	2.57	4.7 ± 0.1	2.8 ± 0.5	1420 ± 120
SMT1 (LMeP)	13	1.48	4.69	2.75	5.2 ± 0.1	3.3 ± 0.2	1390 ± 60
SMT2 (LMeP)	10	1.48	4.68	2.31	4.3 ± 0.1	2.8 ± 0.4	1370 ± 110
FRP1 (RoP)	13	2.43	7.68	2.9	7.6 ± 0.2	11.5 ± 0.9	510 ± 160
FRP2 (RoP)	16	2.22	7.01	2.43	5.9 ± 0.2	9.1 ± 0.5	480 ± 130

Table 5 The physical–mechanical features of representative samples of bricks

Sample	γd (kN/m^3)	γs (kN/m^3)	n (%)	σ (MPa)
Roman Period (RoP)				
TRC1	17.46	25.69	32.2	28.4
TRC2	16.48	26.09	36.0	20.1
FRP1	16.57	27.46	39.6	36.0
FRP2	15.79	26.38	40.2	31.6
Late Medieval Period (LMeP)				
SMT1	17.26	25.89	33.3	21.1
SMT3	15.79	27.26	41.8	23.9
SMT4	16.28	27.46	40.5	19.1
FA1	18.34	27.26	32.4	26.1
FA2	16.57	27.46	39.4	38.8
Modern Period (MoP)				
DUM3	14.91	27.26	45.3	21.9
DUM4	14.71	24.81	40.7	41.5
DUM5	16.77	25.89	35.1	16.2
DUM6	15.49	27.07	42.5	42.2
DUM7	15.89	27.46	42.2	38.9

γd dry bulk density, *γs* specific gravity, *n* porosity, *σ* uniaxial compressive strength (UCS)

grains are detected by OPM. Among the groundmass, the following components were also present: (*i*) brownish to reddish pelitic/marly lumps with frequent calcitic veins and well-preserved *Foraminifera* microfossils (Figs. 4a,b and 5a,b,c) up to 1 cm in grainsize (TRC1 sample); (*ii*) terrigeneous silicoclastic grogs with variable grainsize passing from very fine to medium siltites (Fig. 5d) to coarser-grained sandstone fragments (Fig. 5e); (*iii*) rounded reddish fine-grained fragments containing quartz and muscovite (Fig. 5f), probably referred to the so-called ARFs (Argillaceous Rock Fragments) as defined by Whitbread (1986). Rarely, chert fragments are also detected in the samples of the Roman and Late Medieval Periods.

3.2 XRPD analyses

X-Ray Powder Diffraction analyses (Table 2; SM1) were performed to identify the whole crystalline components, including those which could be difficult to recognise in thin section. It should be noted that the semi-quantitative estimates of minerals are biased to the presence of amorphous (non-crystalline) phases and therefore all the samples show a relatively low crystallinity degree emphasized by the amplitude of the diffractograms' background noise (SM1). The XRPD analyses pointed out the presence of quartz, calcite, feldspar, illite/mica group, clinopyroxene, ± gehlenite and traces of wollastonite; the latter three minerals being the result of new phases after firing. Wollastonite (traces) is only present in the samples DUM2 and DUM4, showing the highest clinopyroxene contest and the lowest values of LOI (1–1.5 wt.%). These are the only two samples where calcite is almost absent (traces, Table 2), and therefore, the highest temperature of firing can be hypothesised (900–1000 °C) whereas for all the other brick samples, the firing temperature should have not exceeded 850–900 °C. The co-presence of gehlenite (which starts to form at temperatures of 800–850 °C at the expense of silica, clay minerals and calcite; Cultrone et al. 2001; Traoré et al. 2003; Gliozzo 2020) and calcite (normally decomposing at that temperature) is mainly due to the inhomogeneity of the grainsize of the used raw materials. According to Allegretta et al. (2016), the reactions which take place along grain boundaries between calcite and clay groundmass are a function of grainsize, other than paste composition, heating rate, duration and redox condition of firing. It is worth to note that, as reported by Cultrone et al. (2001) and Fabbri et al. (2014) calcite starts decomposing at around 700 °C but it can be detected up to 900 °C since decarbonation temperature depends on the grainsize as well as firing conditions. The

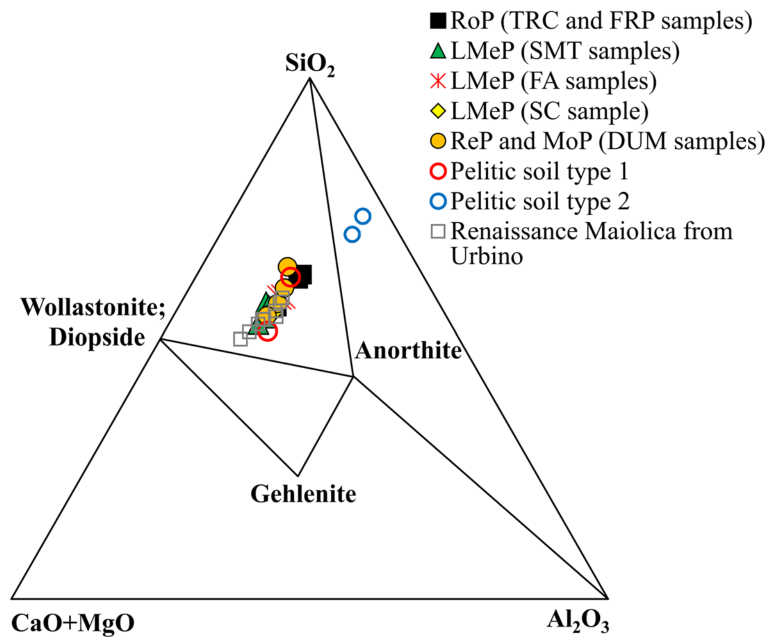

Fig. 6 (CaO + MgO)—Al_2O_3—SiO_2 phase diagram composition of analysed bricks and firing phases, such as wollastonite, diopside, melilite (gehlenite) and plagioclase (anorthite), with relative tie-lines (according to Artioli et al. 2000). Comparisons with Renaissance Maiolica from Urbino (Antonelli et al. 2014) and two types of pelitic soils outcropping near Urbino (Busdraghi 1992) are also reported (Source: the authors)

medium to coarse-grained pelitic/marly lumps (Figs. 4a,b and 5a,b,c) enriched in carbonatic components and also calcite veins and *Foraminifera*, did not completely decompose during the firing process. By contrast, the formation of new phases such as gehlenite during firing is the result of decomposition of the finer-grained carbonate components having higher specific surface areas (Allegretta et al. 2016). As also reported in the literature (*e.g.* Coletti et al. 2023), the coexistence of carbonates, illite/mica group and silicates in ancient brick masonry suggests the absence of good standardisation in the firing processes. The sporadic presence of gypsum (SMT2 and SC1) and zeolites (SMT4, probably analcime for peak at 5.6 Å), detected in the Late Medieval brick samples, is the result of weathering products, *i.e.* secondary phases from decay processes affecting the monuments.

3.3 Chemical composition

The bulk chemical analyses (BCA) of 14 selected samples (major and trace elements; Table 3) show very high LOI (Loss on Ignition) values (7.5–16.6 wt.%) except for two samples from the Cathedral, DUM2 and DUM4, with a LOI of 1–1.5 wt.%. In general, the analysed bricks show a relatively homogeneous composition throughout the four building periods, with variable CaO (12.2—22.3 wt.%) and MgO (3–5.9 wt.%) and quite homogeneous content of Fe_2O_3 (4.2—5.8 wt.%), Na_2O (0.8—1.8 wt.%), K_2O (1.6—3.3 wt.%) and TiO_2 (0.5—0.6 wt.%). CaO + MgO percentage is within 15–26 wt.% (Table 3), generally considered as a Carbonatic Bodies (CBs) cluster for ancient bricks. CBs are, for example, one of the two clusters (the other is the Carbonatic-High Carbonatic Bodies, CHCBs) recognised for bricks from the Early Christian to the Renaissance Periods in the built heritage of the Italian city of Padua (Pérez Monserrat et al. 2022). In the phase diagram (CaO + MgO)-Al_2O_3-SiO_2 (Fig. 6), all the samples of the present study fall within the quartz-anorthite-diopside (wollastonite) compositional triangle (the same field of most of the ancient ceramic and bricks; Artioli et al. 2000; Bianchini et al. 2002, 2006). Concerning trace elements (Table 3), bricks also highlight a relatively homogeneous composition regardless of the historic periods. In the box-plot diagrams (Fig. 7) Rare Earth Elements (REEs) such as La, Ce, Nd and High Field Strength Elements (HFSEs) such as Zr, Nb, Th confirm a narrow and overlapping range of values, suggesting the use, over time (from RoP to MoP) of similar raw materials to produce bricks. It is worth to note that REEs and HFSEs are generally considered those reflecting the original composition of the source rock being the least mobile elements during weathering and other kinds of alteration processes. In Fig. 7 the average values of these elements for bricks of the various historic periods are within 5–15% variability *i.e.* very close to the analytical errors. Comparisons with available literature data (Fig. 6) show that the composition of the investigated bricks falls very

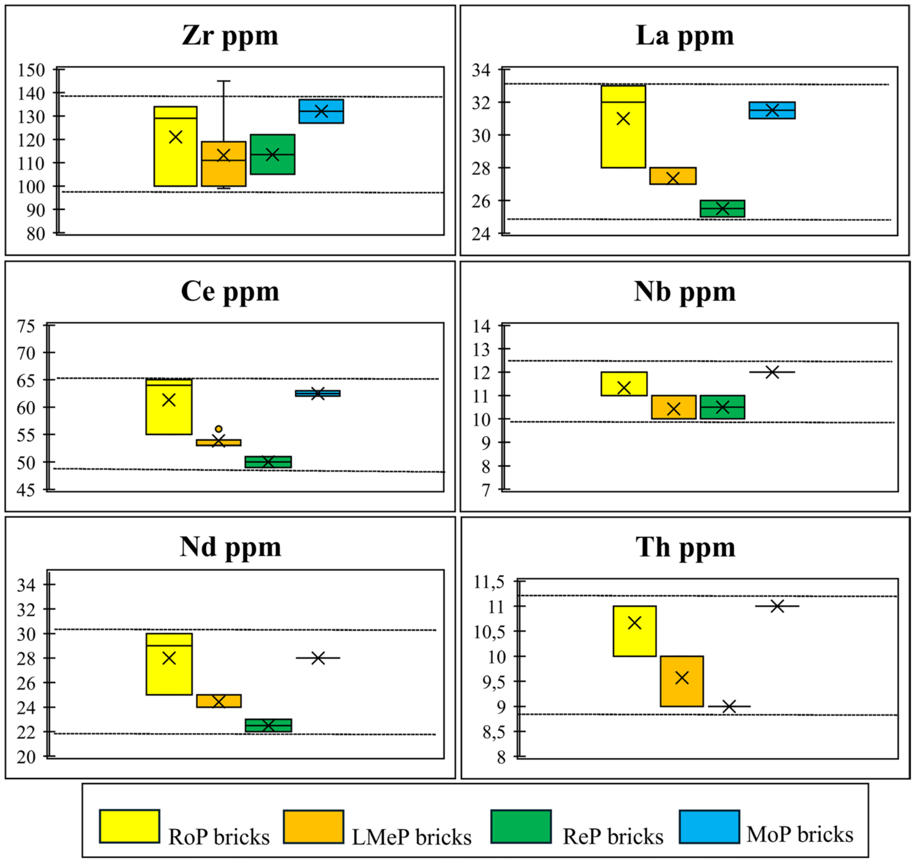

Fig. 7 Box-plots showing some trace element variations for the analysed bricks. The boxes represent the standard 50% of the data whereas the range values are defined by vertical bars (excluding outlier samples as single points, *e.g.* Ce diagram). Median and average values are respectively marked by a black line and a cross inside the boxes (Source: the authors)

close to both the chemical composition of some Renaissance Maiolica from Urbino (Antonelli et al. 2014) and that of the pelitic soil "type 1" (rather than the grey-blue clay-silt "type 2"), detected in some drillings and excavations in the Urbino centre and surroundings (Busdraghi et al. 1992). The main difference in composition between these two soils (Busdraghi et al. 1992) is represented by lower CaO content showed by "type 2" (1—4 wt.%) with respect to the "type 1" level (14–18 wt%) which roughly agrees with the composition of the analysed bricks (12–22 wt.%). "Type 1" soil represents the continental quaternary deposits deriving from the weathering of the Marnoso-Arenacea Formation extensively outcropping in the surroundings of Urbino (AA.VV. 2009). This soil shows extreme variability, both in the areal distribution and the thicknesses, depending on weathering processes and morphological features of the territory. The similarity in major elements and the 5–15% variability of REEs and HFSEs throughout all the investigated bricks is thus compatible with the same geological formation (source rock).

3.4 TL dating

The thermoluminescence (TL) dating of 9 bricks supports the chronology of the construction periods inferred from the historic data. The results are reported in Table 4. The oldest TL dating, which straddles the end of the Roman Empire (FRP1, 510 ± 160 CE and FRP2, 480 ± 130 CE) is related to the little Roman furnace (Fig. 2a,b) located just outside (NW) the historic centre. The bricks sampled from the Late Medieval structures indicate a time interval extending from the second half of the 14th century up to the 15th century: *Santa Maria della Torre* church (Fig. 2a,c) was dated at 1370 ± 110 CE for SMT2 and 1390 ± 60 CE for SMT1 whereas the Albornoz Fortress (Fig. 2a,d) at 1420 ± 120 CE (FA1). The multi-phase construction of the Urbino Cathedral, documented by historic data (Negroni 1993), and mainly linked to damages due to some earthquakes (*i.e.* the seismic events of 1741, 1781 and 1789), is supported by the obtained four TL dating. The bricks referred to a pillar in the Renaissance Period of construction (Fig. 3a,b,c) well correspond to the different depths of sampling (drill cores) of the same pillar (see Materials and Methods and Table 1). Their different dating at 1460 ± 80 CE (DUM1b) and 1560 ± 90 CE (DUM1a) clearly testify to two different building phases. The difference of about one century between the bricks of the inner (DUM1b) and the outer (DUM1a) parts of the same pillar would account for overlapping construction phases of the Cathedral during the Renaissance. The dating of DUM1b at 1460 ± 80 CE is in agreement with some literature data reporting an act of sale of the second half of the 15th century, where an inhabitant of "Villa di Carpineto" (to the West of Urbino) was committed to provide twenty thousand "well made and well fired" bricks to the Cathedral factory by August 1478 (Negroni 1993). Concerning the other samples coming from the reconstructed drum of the dome (18th-19th century), they date at 1780 ± 50 CE (DUM5) and 1800 ± 40 CE (DUM4).

The uncertainties associated with the calculated ages, which range between ± 8% and ± 20%, reflect the accuracy of the equivalent dose evaluation. It depends on the reproducibility of repeated measurements and the precision in the calibration of the radioactive sources; even if in most cases, the uncertainty associated with Equivalent Dose is between ± 3% and ± 7%, in our case, it spans ± 3% and ± 18%.

3.5 Physical–mechanical features

Fourteen brick samples were analysed to define their volumetric parameters (Table 5). The obtained data do not show significant differences between the bricks related to the various historic periods. The dry bulk density (γd) of the Late Roman Period samples is moderately variable (from 15.8 to 17.5 kN/m^3), quite similar to that of the bricks of the Late Medieval Period (16.8 kN/m^3). Bricks of the Modern Period (eighteenth-nineteenth centuries, Urbino Cathedral) show a range of γd between 14.7 to 16.8 kN/m^3.

The specific weight (γs) is very similar for all the analysed samples, with the Roman bricks showing a range between 25.7 and 27.4 kN/m^3, the Medieval bricks from 25.9 to 27.5 kN/m^3 and those of the Modern Period from 24.8 to 27.5 kN/m^3. The total porosity (n) values are similar for the Roman (from 32 to 40%) and Medieval (from 32 to 42%) brick samples, whereas it is slightly higher for those of the Modern Period (from 35 to 45%). The distribution of porosity values and their relationship with the dry bulk density (Table 5), due to the substantial homogeneity of specific gravity values for almost all samples, shows, accordingly, a close inversely proportional relationship. Concerning the values of Uniaxial Compressive Strength (σ; UCS), they are between 20 and 36 MPa for the Roman bricks, from 19 to 39 MPa for the Medieval bricks, and from 16 to 42 MPa for bricks of the Modern Period. Three samples (DUM4, DUM6, DUM7) of the Modern Period (eighteenth -nineteenth centuries), which were used in an important architectural structure (*i.e.* the Cathedral), have the highest UCS (between 38.9 and 42.2 MPa) among all the investigated bricks.

4 Summary and discussion

The analysis of the representative bricks from various architectural structures of the historic centre of Urbino contributes to defining several archaeometric aspects related to pyrotechnology, manufacturing techniques, and the selection of raw materials over time. Moreover, TL dating strongly supports the historical data on the building periods found in the literature. The bricks of the Late Roman Period are characterised by a relatively low percentage of groundmass and a high vol.% of poorly sorted and medium- coarse-grained components, consisting of quartz, K-feldspar, plagioclase, micas, chert, pelitic/marly lumps, siltites, oxidized fragments and, found only in these samples, rounded reddish clasts containing quartz and muscovite (ARFs; Fig. 5f). All these mineralogical and textural features seem to suggest rough techniques of dough processing, mixing and grinding of the various components before firing, even if, chemical analyses (Table 3) show a rather compositional homogeneity among the samples. The orange colour of the bricks (Fig. 4a) suggests a firing process with good oxygenation and a continuous air exchange inside the furnace. TL dating of the bricks coming from the Roman furnace (Table 4) indicates that it was still working until the fifth-sixth century.

The bricks coming from the rampart of the *Santa Maria della Torre* church (Table 4) that was part of the Medieval city walls, are poorly sorted, with a temper content between 20 to 35 vol.%, consisting mainly of quartz, K-feldspar, plagioclases, micas, chert, pelitic/marly lumps and arenite fragments. These latter represent an additional type of temper recognized in the investigated samples from the Late Middle Age onwards. The texture of the samples observed under the optical polarized microscope point out an improvement in processing and preparation techniques of the dough with respect to the bricks of the Roman Period. This is emphasised by the relatively low content of clasts and better sorting, although a poor homogenization treatment of the raw material is still present (the paste was not well broken). In some samples, secondary minerals such as gypsum and analcime (zeolite) were detected by microscope observations and XRPD analyses (Table 2), which were deposited in the pores and cracked by weathering processes. The Late Medieval bricks coming from the Albornoz Fortress and the walls of the former Dominican Convent show a common texture reflecting similar dough preparation and firing techniques. These Late Medieval bricks are characterised by a poorly sorted paste consisting of quartz, mica, K-feldspar, plagioclase, pelitic/marly lumps, terrigenous silicoclastic fragments (arenites in FA1 and both siltites and arenites in FA2 and SC1). The samples of Albornoz Fortress show a lack of homogeneity in the optically active groundmass, due to different colour gradations, indicating the use of raw materials that have not undergone an adequate homogenisation treatment before firing.

The bricks from the Cathedral belong to two different historic periods, depending on the different phases of the construction of the structure: the Renaissance and the Modern building period (Table 4). DUM1a and DUM1b (third pillar of the left nave) and DUM2 (pediment of the façade) are referred to the Renaissance building Period, as also testified by the TL dating of the different depths of the drill core of the pillar (1460 ± 80 CE and 1560 ± 90 CE). By contrast, DUM4 and DUM5 samples (as well as DUM3, DUM6, and DUM7), coming from the bricks of the reconstructed drum of the dome, historically dated to the building period of the eighteenth-nineteenth centuries, were coherently dated by TL at 1780 ± 50 CE and 1800 ± 40 CE. The brick samples of the Cathedral consist of the same mineralogical/textural components as those from the Late Medieval Periods but show a higher degree of sorting of the dough. The yellowish colour of the optically inactive groundmass of the DUM2 and DUM 4 samples (Fig. 4d) suggests firing conditions in a reducing atmosphere, where oxidation is prevented by the absence of oxygen (Ingham 2013).

The major-trace elements variation of all the investigated bricks shows a rather homogeneous composition, and the (CaO + MgO) percentage within 15–26 wt.% closely matches with Carbonatic Bodies (CBs) cluster already recognised for ancient bricks (Pérez Monserrat et al. 2022). In the phase diagram (CaO + MgO)-Al_2O_3-SiO_2 of Fig. 6, all the bricks fall within the quartz-anorthite-diopside (wollastonite) triangle, showing similarity with the local pelitic soil "type I" reported by Busdraghi et al. (1992) and with the compositions of some Renaissance Maiolica from Urbino (Antonelli et al. 2014). This suggests the marly/clayey arenitic sediments deriving from the weathering of the Marnoso-Arenacea Formation, outcropping in the surroundings of Urbino, as the best candidate raw materials. In particular, the hillside facing West of both the present-day *La Piantata* district and the Roman kiln (North of Urbino; Fig. 2a) is one of the areas from which the raw material for manufacturing bricks could have been most likely exploited since it is characterized by a large amount of continental quaternary deposits fed by the Marnoso-Arenacea Formation. The whole western and northwestern slopes and gullies in the surroundings of Urbino are good candidates for brick raw materials. In addition, some historic documents of the second half of the 15th century involving inhabitants of those areas with a commitment to supply bricks to the Cathedral factory (Negroni 1993) seem to confirm the above geological constraints. This hypothesis is also supported by the presence in this area of the Roman furnace (Fig. 2a), certainly built near the place from which the raw materials could be obtained. It is plausible to hypothesise that these deposits could have been exploited for the production of bricks not only during the Roman and Late Roman Periods but also later. In any case, suitable deposits deriving from the weathering of some outcrops of the Marnoso-Arenacea Formation and thus an ideal site of exploitation of raw materials also occur in the *Schiavonia-Castagneto* valley (Falcioni et al. 2024), an area located southeast of the historic centre, between the town and the San Bernardino hill where, around the mid-1800s, the brick factory *Fornace Volponi*, was founded. Unfortunately, there are no documents available to exactly reconstruct the raw material areas which supplied the manufacturing of this furnace, which was decommissioned between 1971 and 1974 (Agostinelli et al. 2007).

Concerning firing temperature and condition, it is important to note that we found gehlenite at least in one brick sample for each building period and thus temperatures of at least 850–900 °C should have been reached, when CaO from the calcite breakdown react with Al_2O_3, MgO, and SiO_2 from the clay minerals to originate clinopyroxene and gehlenite. We could explain the co-presence of gehlenite and calcite as the result of the poorly sorted raw materials and the lack of standardised firing conditions. The higher specific surface areas of the finer carbonate components increasing their contact surfaces with the clay matrix, allowed new phases such as gehlenite to form during firing, whereas the carbonate fractions of the pelitic/marly lumps persisted (Allegretta et al. 2016; Coletti et al. 2023). The presence of gehlenite can also be associated with the compositional inhomogeneity of the original material, with the failure to achieve thermodynamic equilibrium conditions (Artioli et al. 2000), other than kinetic reasons during firing such as the rate of the temperature increase (Riccardi et al. 1999). Calcite appears to diminish to trace amounts only in the Modern bricks of the Cathedral, thus suggesting that the firing temperatures, although reaching 850 °C (gehlenite), never produced complete $CaCO_3$ breakdown. Some additional explanations of the coexistence of calcite and gehlenite in the investigated samples could be however deepened in future works. Only for the DUM2 and DUM4 samples, having traces of wollastonite, the highest content of clinopyroxene, nearly absence of calcite, and the lowest LOI, a firing temperature up to 900–1000 °C could have been reached.

The physical–mechanical features, the Uniaxial Compressive Strength (UCS) values (Table 5) are comparable to those of full-bricks produced nowadays *e.g.* between 15 to 50 MPa (data from T2D s.p.a. 2023) highlighting the relatively good production quality of the bricks used in the historic centre of Urbino in ancient times. Large variability in the UCS values (depending on firing temperature) even in the buildings of the same periods is probably due to the lack of standardization of the firing temperature. Nevertheless, the highest UCS values are shown for some bricks from the Modern Period building of the Cathedral (DUM4 and DUM6, 41.5 and 42.2 MPa respectively) emphasizing a general trend of increasing physical–mechanical quality with time.

5 Conclusions

This interdisciplinary study highlights the historic importance of bricks as building material of Urbino already considered the "city of bricks" by Baldi (Baldi 1580; Siekiera 2010) and Mazzini (1982). In this way, the archaeometric investigations here reported, coupled with mapping the possible local sites of brick manufacturing and the areas of supplying of the raw materials, support and valorise the brick material culture of Urbino. The nine TL datings of bricks (although with relatively high errors) yielded a time interval from Late Roman to the 18th-19th century, roughly confirming the historic periods of the architectural building phases of the city and ruling out the re-use of bricks from one building to another through time. TL dating of the remnants of the Roman kiln (FRP1 and FRP2) yielded a younger age (fifth—sixth century) than previously thought from the available archaeological and historic data (third century; Ermeti 1993). This would confirm the use of the furnace also during the Late Roman Period for the local production of bricks and tiles as also witnessed by the defensive walls built in the highest hill of the Roman city in the same historic period (Luni and Ermeti 2001).

A slight to medium improvement and refinement in preparation techniques and processing (grinding and mixing) of the brick paste (clays and temper) before firing, as well as the development of more homogeneous mixtures, were emphasised with time. The trend to produce bricks with increasingly better quality is supported by the decreasing percentage of the temper, associated with an improvement in the degree of sorting achieved from the Late Roman Period up to the eighteenth-nineteenth centuries. The progressive enhancement in the production techniques of bricks is also confirmed by the results of physical–mechanical tests (mainly the UCS; Table 5): DUM4 and DUM6 coming from the eighteenth-nineteenth centuries building phase of the Cathedral, show the highest UCS value (*ca.* 42 MPa) among the investigated samples. DUM4 and DUM 2 (for which UCS is not available) show mineralogical constraints (traces of wollastonite and the nearly absence of calcite), indicating a higher firing temperature up to 900–1000 °C, whereas for all the other investigated bricks, the firing temperature should not have exceeded 850–900 °C. However, it is worth to note that even these bricks of the Modern Period show a large variability of the UCS (between 16 to 42 MPa; Table 5), thus confirming that the production of the highest-quality and homogeneous bricks was also difficult in the eighteenth-nineteenth centuries.

The main raw material for the Urbino bricks is the marly/clayey/arenitic sediments deriving from the weathering of the Marnoso-Arenacea Formation, extensively outcropping in the surroundings of the city. The presence of abundant arenite grains as temper only in the bricks from the Late Medieval Period onwards could be related to possible variations in time of different outcrops of the above-mentioned formation (natural lithological variability of the geological formation concerning the pelite/arenite ratio), which supplied the main raw material. The best candidate supply areas could have been some peripheral slopes located to the west and northwest of Urbino, where some constraints of manufacturers supplying bricks to the Cathedral factory were also found, as act of sale. Alternatively, clues for the provenance of the raw materials may also come from the area to the southeast of the historic centre (*i.e. Schiavonia-Castagneto* area) because it may not be random that the *Fornace Volponi* brick factory, successively working since the middle of 1800s up to the second half of the 20th century was just located there.

The following final remarks can be taken home in the framework of general relevance for fired bricks in the built heritage:

- TL dating coming from different building periods of a historic centre may confirm the chronology of the urbanisation phases, excluding or not any kind of reuse of ancient bricks in younger architectural structures;
- the coupled approach of (*i*) searching the local raw materials (geological formations) for bricks and (*ii*) mapping possible local furnaces through time of an urbanised area allows for reinforcing and better defining the brick material culture in the architectural framework;
- the reaction behaviour of temper grains and clay matrix is dominated by disequilibrium conditions, with different reacting subsystems, especially for

ancient fired bricks of the architectural heritage, where the inhomogeneity of the raw materials and the absence of a good standardisation in the production processes can be very common;
- mineralogical (OPM and XRPD), chemical and physical–mechanical analyses not only give information on the brick components (raw material), pyrotechnological processes and quality but could also account for the state of conservation of the building materials themselves;
- the knowledge of the area of provenance of the raw materials used for ancient bricks, especially when dealing with UNESCO world heritage sites, is of paramount importance when restoration (replace) of damaged (chemically and/or physically degraded) bricks will need, looking for present-day fired bricks manufactured with similar components, thus producing similar aesthetic and physical features.

Abbreviations

UNESCO	United Nations Educational, Scientific and Cultural Organization
TL	Thermoluminescence
RoP	Roman Period
LMeP	Late Medieval Period
ReP	Renaissance Period
MoP	Modern Period
OPM	Optical Polarizing Microscopy
XRPD	X-Ray Powder Diffraction
ICP-OES	Inductively Coupled Plasma-Optical Emission Spectrometry
ICP-MS	Inductively Coupled Plasma-Mass Spectrometry
REE	Rare Earth Elements
MAAD	Multiple Aliquot Additive Dose
De	Equivalent Dose
RT	Room Temperature
ISRM	International Society for Rock Mechanics
UCS	Uniaxial Compressive Strength
EN	European Norm
LOI	Loss on Ignition
HFSE	High Field Strength Elements
CE	Christian Era
vol.	Volume
TSA	Thin Section Analyses
BCA	Bulk Chemical Analyses
PMP	Physical–Mechanical Properties
DL	Detection Limit

Supplementary Information

The online version contains supplementary material available at https://doi.org/10.1186/s43238-025-00233-9.

Supplementary Material. SM1 – Representative X Ray Powder diffractograms of the investigated bricks. Abbreviations of minerals: F = feldspar, Q = quartz, C = calcite, Px = clinopyroxene, I/M Illite/mica group, Gy = gypsum, G = gehlenite, W = wollastonite.

Acknowledgements

We are grateful to: Engineer Diego Talozzi, who permitted sampling of some brick drill cores of the Cathedral and Paolo Tomassini and Costantina Di Tizio for sampling of some bricks of the Late Medieval Period. XRPD analyses and interpretation of diffractograms were done by Michele Mattioli, who sincerely thanks. We are also grateful to two anonymous reviewers and the Editor, whose comments and suggestions strongly improved the manuscript.

Authors' contributions

Conceptualization: PS, FV, GT, MT and AR; methodology: PS, FV, GT, MT, LP, AG and AR; investigation: PS, FV, GT, MT, LP, AG and AR; writing-original draft preparation: PS, FV and AR; writing-review and edit¬ing: PS, FV, GT, MT, LP, AG and AR; visualization: PS, FV and AR; supervision: PS, FV, GT, MT, LP, AG and AR; funding acquisition: PS. All authors have read and agreed to the published version of the manuscript. All authors read and approved the final manuscript.

Funding

This research was funded by Department of Pure and Applied Sciences, University of Urbino Carlo Bo, "P.Santi, DISPEA 2024".

Data availability

Data will be made available on reasonable request.

Declarations

Ethics approval and consent to participate

Not applicable.

Competing interests

The authors declare that they have no competing interests.

Received: 1 April 2025 Revised: 23 September 2025 Accepted: 27 September 2025
Published online: 28 October 2025

References

AA.VV. 2009. *Carta Geologica d'Italia 1:50.000, Foglio 279 "Urbino"*. ISPRA Roma.
Agnati, U. 1999. Urvinum Mataurense. In *Per la storia Romana della Provincia di Pesaro e Urbino*, ed. Ulrico Agnati, 19–108. Roma: L'Erma di Bretschneider.
Agostinelli, M., P. Clini, N. Lancioni, R. Quattrini, and G. Sabbatini. 2007. The Volponi's kiln in Urbino. Industrial archaeology and landscape in the cradle of the Renaissance. Documentation, survey and drawing. In *Proceedings of XXI International CIPA Symposium*, 01–06 October 2007, Athens, Greece.
Aitken, M.J. 1985. *Thermoluminescence dating*. London: Academic Press.
Allegretta, I., D. Pinto, and G. Eramo. 2016. Effects of grain size on the reactivity of limestone temper in a kaolinitic clay. *Applied Clay Science* 126: 223–234.
Antonelli, F., A.L. Ermeti, L. Lazzarini, M. Verità, and G. Raffaelli. 2014. An archaeometric contribution to the characterization of Renaissance maiolica from Urbino and a comparison with coeval maiolica from Pesaro (the Marches, Central Italy). *Archaeometry* 56 (5): 784–804.
Artioli, G., G. Bagnasco Gianni, S. Bruni, F. Cariati, P. Fermo, S. Morin, and U. Russo. 2000. Studio spettroscopico della tecnologia di cottura di ceramiche etrusche dagli scavi di Tarquinia. In *Atti I° Congresso di Archeometria*, ed. Martini M., 335–349. Bologna: Patron.
Artioli, G., M. Secco, and A. Addis. 2019. The vitruvian legacy: Mortars and binders before and after the Roman world. *EMU Notes in Mineralogy* 20 (4): 151–202.
Ashurst, John, and Nicola Ashurst. 1988. *Brick, terracotta and earth. Practical Building Conservation: English Heritage Technical Handbook, 2*. Aldershot: Gower Technical Press.
Baldi, B. 1580. Encomio della Patria a Francesco Maria II duca di Urbino. In *Urbino 1706*, ed. Angelo Monticelli.
Bianchini, G., A. Martucci, and C. Vaccaro. 2002. Petro-archaeometric characterization of "cotto ferrarese": Bricks and terracotta elements from historic buildings of Ferrara. *Periodico di Mineralogia* 71 (Special Issue): 101–111.
Bianchini, G., E. Marocchino, A. Moretti, and C. Vaccaro. 2006. Chemical-mineralogical characterization of historical bricks from Ferrara: an integrated bulk and micro-analytical approach. In *Geomaterials and Cultural Heritage*, eds. M. Maggetti and B. Messiga, 257: 127–140. London: GSL, Special Pubblication.
Busdraghi, P., S. Vannucci, and F. Veneri. 1992. Le materie prime utilizzate in epoca Rinascimentale per la fabbricazione dei mattoni della cinta muraria di Urbino. In *Atti Convegno Scienza e Beni Culturali*, 655–664. Bressanone: Libreria Progetto.

Coletti, C., L.P. Cesareo, J. Nava, L. Germinario, L. Maritan, M. Massironi, and C. Mazzoli. 2023. Deterioration effects on bricks masonry in the Venice Lagoon cultural heritage: study of the main façade of the Santa Maria dei Servi church (14th century). *Heritage* 6: 1277–1292. https://doi.org/10.3390/heritage6020070.
Cultrone, G., C. Rodriguez-Navarro, E. Sebastian, O. Cazalla, and M.J. De La Torre. 2001. Carbonate and silicate phase reactions during ceramic firing. *European Journal of Mineralogy* 13 (3): 621–634.
EN 1926. 2007. *Natural stone test methods - Determination of uniaxial compressive strength*. London: BSI.
Ermeti, A.L. 1993. La ceramica tra XIII e XIV secolo a Urbino. Materiali dal "butto" in località Bivio della Croce dei Missionari. *Bollettino Museo Internazionale Ceramiche Faenza* III-IV: 89–127.
Fabbri, B., S. Gualtieri, and S. Shoval. 2014. The presence of calcite in archaeological ceramics. *Journal of the European Ceramic Society* 37 (7): 1899–1911.
Falcioni, A., W. Monacchi, and V. Mosconi. 2024. *Girolamo di Tommaso Galli. Ceramista. I documenti d'archivio*. Urbino: Monacchi.
Gliozzo, E. 2020. Ceramic technology. How to reconstruct the firing process. *Archaeological and Anthropological Sciences* 12: 260.
Ingham, J.P. 2013. *Geomaterials under the microscope*, 192. Elsevier: Academic Press.
ISRM. 1979. Suggested methods for determining the uniaxial compressive strength and deformability of rock materials. *International Journal of Rock Mechanics and Mining Sciences* 16: 135–140.
ISRM. 1981. Suggested methods for determining water content, porosity, density, absorption and related properties. In *Rock Characterization Testing and Monitoring: ISRM Suggested Methods*, ed. E.T. Brown, 81–88. Oxford: Pergamon Press.
Ligi, B. 1938. *Memorie ecclesiastiche di Urbino*. Urbino: Cappelli.
Luni, M. 1985. Per la topografia storica di Urvinum Mataurense (Urbino). Appendice II. *Atti della Accademia Nazionale dei Lincei* XXXVI: 400–407.
Luni, M. 1986. Urvinum Mataurense (Urbino). Dall'insediamento Romano alla città Medievale. In *Il Palazzo di Federico da Montefeltro, restauri e ricerche*, 11–49. Urbino: Quattroventi.
Luni, M., and A.L. Ermeti. 2001. Le mura di Urbino tra tardo antico e Medioevo. In *Atti del I Congresso Naz Archeologia Medievale, Pisa*, 41–50. Firenze: All'Insegna del Giglio.
Martini, M., and E. Sibilia. 2001. Radiation in archaeometry: Archaeological dating. *Radiation Physics and Chemistry* 61: 241–246.
Mazzini, F. 1982. *I mattoni e le pietre di Urbino*, 609. Urbino: Argalia.
Mercando, L. 1985. Urbino (Pesaro). Necropoli romana: Tombe al Bivio della Croce dei Missionari e a San Donato. *Atti della Accademia Nazionale Dei Lincei* XXXVI: 109–121.
Munsell, A.H. 1994. *Munsell soil color charts*. New Windsor: Macbeth.
Negroni, F. 1993. *Il Duomo di Urbino*. Urbino: Accademia Raffaello.
Negroni, F. 2005. *Appunti su alcuni palazzi e case di Urbino*. Urbino: Accademia Raffaello.
Pérez Monserrat, E.M., L. Maritan, and G. Cultrone. 2022. Firing and post-firing dynamics of Mg- and Ca-rich bricks used in the built heritage of the city of Padua (northeastern Italy). *European Journal of Mineralogy* 34: 301–319.
Prescott, J.R., and J.T. Hutton. 1994. Cosmic ray contribution to dose rates for luminescence and ESR dating: Large depths and long-term time variations. *Radiation Measurements* 23: 497–500.
Riccardi, M.P., B. Messiga, and P. Duminuco. 1999. An approach to the dynamics of clay firing. *Applied Clay Science* 15: 393–409.
Rovida, A., M. Locati, R. Camassi, B. Lolli, P. Gasperini, and A. Antonucci. 2022. *Catalogo Parametrico dei Terremoti Italiani (CPTI15) Versione 4.0*. Roma: Istituto Nazionale di Geofisica e Vulcanologia (INGV). https://doi.org/10.13127/cpti/cpti15.4.
Rowland, I.D., and T.H. Howe 1999. *Vitruvius: Ten Books on Architecture.* Cambridge: Cambridge University Press.
Santi, P., F. Veneri, G. Tonelli, A. Renzulli, F. Antonelli, and M. Tramontana. 2019. The ancient quarrying areas of the sandstones used in the UNESCO historical centre of Urbino (Marche, Italy) as inferred from geological, petro-chemical and physical-mechanical investigations. *Italian Journal of Geosciences* 138 (3): 456–470.
Santi, P., M. Tramontana, G. Tonelli, F. Veneri, and A. Renzulli. 2021. The historic centre of Urbino, UNESCO World Heritage (Marche Region, Italy): An urban-geological itinerary across the building and ornamental stones. *Geoheritage* 13: 86.
Siekiera, A. 2010. Bernardino Baldi: Descrittione del Palazzo Ducale di Urbino. Alessandria: Edizioni dell'Orso.
T2D s.p.a. 2023. *Guida ai Mattoni Pieni e sue applicazioni.* T2D. https://t2d.it/news/mattoni-pieni-guida-a-tipologie-e-caratteristiche-tecniche.
Traoré, K., T.S. Kabré, and P. Blanchart. 2003. Gehlenite and anorthite crystallization from kaolinite and calcite mix. *Ceramics International* 29 (4): 377–383.
UNESCO. 1998. *Historic Centre of Urbino.* 1998. http://whc.unesco.org/en/list/828/.
Whitbread, I.K. 1986. The characterisation of argillaceous inclusions in ceramic thin sections. *Archaeometry* 28 (1): 79–88.
Zimmermann, D.W. 1971. Thermoluminescence dating using fine grains from pottery. *Archaeometry* 13: 29–52.

Publisher's Note